IASS 2020/21 SURREY 7
International Conference on Spatial Structures 2020/21

Proceedings of the IASS Annual Symposium 2020/21 and the 7th International Conference on Spatial Structures
Inspiring the Next Generation
23 – 27 August 2021, Guilford, UK
S.A. Behnejad, G.A.R. Parke and O.A. Samavati (eds.)

D-Nets on rotational surfaces
Equilibrium gridshell layout, symmetric to the principal stress directions

Eike SCHLING*, Jonas SCHIKORE[a], Thomas OBERBICHLER[b]

*The University of Hong Kong, Department of Architecture,
Knowles Building 4/F 413, Pokfulam Road, Pokfulam, Hong Kong
schling@hku.hk

[a] Technical University of Munich, Department of Architecture, Chair of Structural Design
[b] Technical University of Munich, Department of Civil Engineering, Chair of Structural Analysis

Abstract
This paper presents a novel topology for gridshells symmetric to the principal stress directions. This diagonal layout (D-Net) allows to distribute forces evenly across neighbouring members and create equilibrium states for compression- (or tension-) only gridshells, through its orthotropic behaviour. We derive a formula for the D-Net directions and present a computational workflow to calculate their paths on NURBS surfaces under given loads and supports. The workflow is conducted using isogeometric analysis (IGA) that continuously evaluates the stress field over the smooth geometry. In this initial investigation, we focus on rotational surfaces for compression-only and mixed (compression and tension) gridshells. The results are verified with a series of archetypical design shapes and Finite Element analysis. We compare the structural behaviour of three gridshells, equilateral, principal-stress and D-Net, evaluating the holistic load-bearing behaviour under four load-cases. Finally, we discuss the practical challenges for D-Net design and its potential for architecture. The research gives a holistic assessment of theory, design and structural behaviour, and opens the doors to a novel topology for gridshell design, that naturally follows the flow of forces.

Keywords: Gridshells, Isogeometric Analysis, Topology Optimization, Force Equilibrium, Principal Stress Directions

1. Introduction
It is widely accepted in the architectural, engineering and the applied-geometry community that the principal stress (PS) vector fields encode the optimal topology for gridshells (Michell 1904; Mitchell 2013; Tam and Mueller 2015). Such trajectories indicate the path of maximum/minimum in-plane stresses (tension and compression) and vanishing shear stress. A quadrilateral gird structure designed along these vector fields will be at equilibrium, i.e. its quads won't tend to skew (Michalatos and Kaijima 2014; Pellis and Pottmann 2018).

When used for gridshell construction, we can expect efficient use of material along the shortest path of loads to the supports, and almost no stress of the diagonal bracing (for the particular load case). The paths of principal stress have inspired architectural design from the ribbed plates of the Gatti Wool Mill 1951 (following the principal bending moments), to the gridshell designs of Brinebath in Bad Dürrheim 1987 or the CIAB Pavilion 2013 (approximating the principal stress trajectories) (Figure 1).

Figure 1: Architectural designs using the Principal Stress Directions.
A: The concrete ribbed floor slabs of Gatti Wool Mill, 1951, by Pier Luigi Nervi following the principal bending moments.
B: The hanging timber gridshell of the Solemar Brinebath in Bad Duerrheim, 1987.
C: The multi-layered system of steel pipes of the CIAB Pavilion, Beijing, 2013 by Zaha Hadid Architects.

There are, however, constructive disadvantages to a PS layout. An orientation of structural elements along the maximal and minimal stress leads to a heterogeneous distribution of stress, in which the member taking the maximal compression is prone to buckling, while the secondary direction is not utilized to its full potential. This is usually resolved by creating a hierarchy of members (Figure 1, B).

Many gridshells profit from a homogenous layout with standardized profiles, not only for its aesthetic value of omitting a hierarchy of elements but also for consideration of the fabrication and construction process: In the case of the strained timber gridshells of Frei Otto (Figure 3, A) it was of utter importance, that all members were equally elastic to be bent into their funicular shapes (Happold and Liddell 1975). This posed the question of alternative gridshell topologies, which allow for a homogenous distribution of stress in neighbouring members.

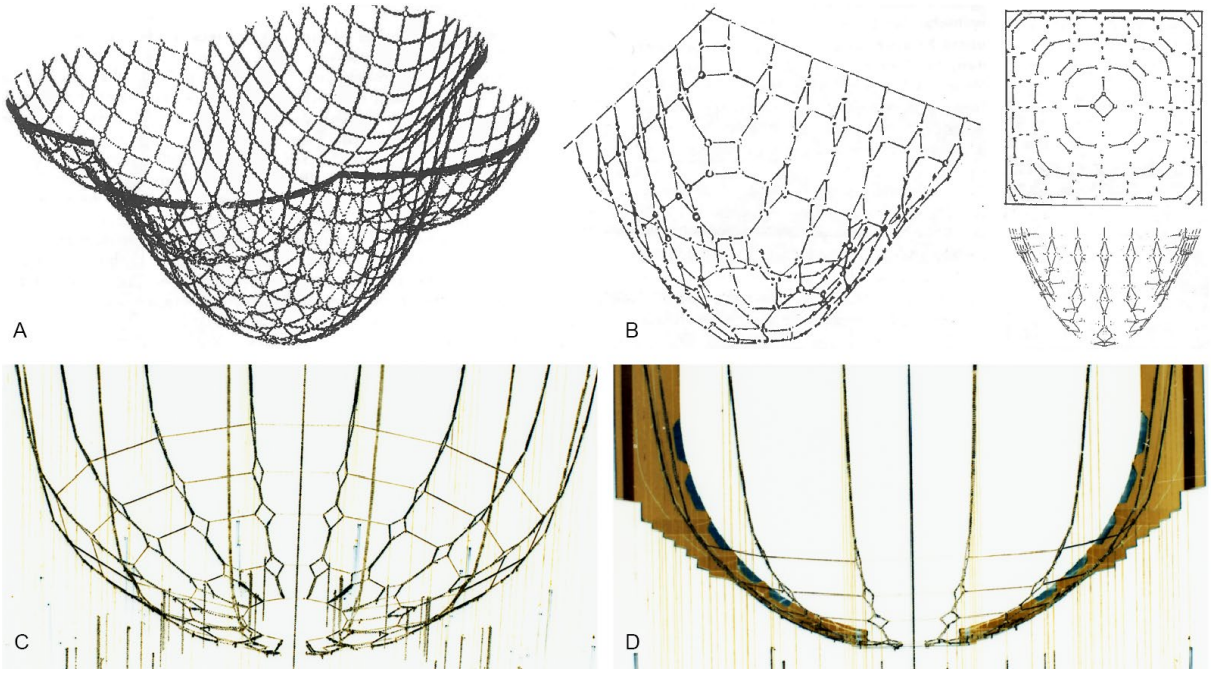

Figure 2: Hanging-chain models of the Institute for Lightweight Structures (IL).
A: An equilateral grid under self-weight, will find an equilibrium shape. Diagonally oriented meshes exhibit a gradual elongation towards the supports. B: This behaviour was used to visualize the proportion of meridian and ring stresses (Hennicke 1974). C/D: The analytical model of Pantheon in Rome (Rainer Barthel).

Frei Otto and his team systematically investigated funicular equilateral grids, using physical (and digital) hanging chain models to find their equilibrium shape and topology (Figure 2, A). These experiments created a world of design solutions (Hennicke 1974). The IL team also discovered a particular effect to analyse domes and shells that is taking advantage of the kinematic behaviour of diamond quads, acting as a local mechanism and naturally taking on the equilibrium shape of forces applied to their four nodes. Inserting a diamond mesh (diagonal to the principal stress directions) at each node of a regular grid (B) beautifully visualize the ratio of meridian and ring forces. For a semi-sphere, such as the analytical model of the Pantheon (C, D), the diamonds show the gradual decrease of ring forces from the pol upwards. Above 52°, all diamond meshes are closed.

We are interested in the design potential of this particular effect. We propose a novel gridshell topology of diagonal nets (D-Nets) that follow a path symmetric to the principal stress directions. Such a topology does not only distribute stress evenly across neighbouring members, its orthotropic behaviour allows for equilibrium states for compression/tension-only structures with minimal need for bracing. Additional D-Nets visualize the ratio of forces and create a natural flow of members towards the supports.

Figure 3: Gridshells that display a gradual incline of diagonal members, naturally adjusting to the stress caused by dead-load. A: The experimental timber gridshell in Essen by Frei Otto 1976. B: King's Cross Station Extension in London, 2013. C: Asymptotic Canopy, Intergroup Hotel in Ingolstadt, 2020 (Schling and Schikore 2020).

In this paper, we first recapitulate the fundamentals of stress distribution on smooth shells using Mohr's circle. We highlight its relevance for the design and construction of quadrilateral gridshells, and introduce the concept of orthotropic behaviour of quads. We then deduce a simple formula to calculate the direction of principal-symmetric, diagonal nets, and introduce a novel analytic method, using IGA to iteratively find the diagonal equilibrium paths for D-Nets based on the local direction and ratio of principal stresses. This method allows the architect to design a shell first (by specifying surface, loads and supports), and then generate a diagonal network that visualizes the flow and ratio of forces.

We verify our new method through modelling and assessing a series of rotational surfaces. We specifically compare the structural behaviour of three gridshell domes, on equilateral, one principal-stress, and one D-Net, under varying loads, and evaluate their load-path and eigenforms. Finally, we give an outlook of the challenges and potentials of D-Net design.

2. Fundamentals

Our research combines two fundamental principles: the **orthotropic kinematic** behaviour of quads, and the principal stresses trajectories, illustrated by **Mohr's Circle**. We are particularly interested in the relationship of principal stress to a diagonal quad layout and its potential to alternative equilibrium states.

2.1 Orthotropic kinematic behaviour of quads

A quad itself is kinematic, considering it is hinged at the nodes and able to transmit tension and compression. It is statically undetermined and creates a local kinematic mechanism with **orthotropic behaviour (**Figure 4, B1): If a rhombus is compressed in the vertical direction, it will naturally expand in the horizontal direction, and vice versa. The relationship of the vertical and horizontal forces are dependent on the particular proportion angle of the diamond. We take advantage of this behaviour, by aligning a diamond-grid symmetric to the principal stress trajectories, so that principal stress 1 and 2 are at equilibrium at any node.

2.2 Mohr's circle

The principal stress trajectories display the natural flow of forces through any structural element, such as a continuous shell, for a particular load and support scenario. They are always perpendicular to each other, indicating the direction and value of the maximum and minimum stress at any point on this surface. Mohr's circle offers a graphical representation of stress components based on the two principal trajectories (Figure 5, A). The two principal stress n_1 and n_2 are plotted along a horizontal axis σ, and thus define a circle C with centre P at their midpoint. This circle graphically provides all other stresses σ and shear stresses τ based on their deviation angle μ from the first principal trajectory n_1. The maximum shear occurs at $\mu = 45°$ (located at the highest and lowest points on the circle, $2\mu = 90°$). The shear stress vanishes at the PS-directions, $\mu = 0°$.

The PS directions can be applied to the structural layout of gridshells, considering a homogeneous self-weight across the shell. In theory, if all members are aligned with the principal stress trajectories, the grid will not suffer distortion and remain stable with minimal bracing.

In practice, loads are variable and so are the principal stresses. Any gridshell requires a minimum amount of bracing against asymmetric loads like wind or snow. Nonetheless, minimizing the shear stress in a gridshell allows the designer to use fewer bracing elements of minimal thickness, but also significantly reduces the stress in the remaining grid, as loads are not carried back and forth through the structure.

3. Methods

In the following section, we first deduce a **formula for D-Net trajectories**. We then present an **analytical method** using IGA, to compute the principal stress on a previously defined surface and iteratively draw the D-Net paths based on our formula. (A simple funicular method of form-finding rotational diagonal hanging nets was omitted from this paper to meet the 12 page maximum).

3.1 Formula for D-Net trajectories

To find the trajectories of D-Nets, we use a rectangular portion of the continuous shell of size $\boldsymbol{x} \times \boldsymbol{y}$ that is aligned with the principle stress directions. We overlay this portion with one mesh of a respective quadrilateral grid (Figure 4) and assume that this grid is subject to the same surface loads, but concentrated in its nodes. From this diagram we deduce two[1] orientations for an equilibrium state:

A: The grid is **aligned with the principal stress trajectories**. The resultant forces are simple. The vertical member force F_A will carry the full load N_1 [kN], which is the resultant of the membrane force n_1 [kN/m] of the respective element width x. F_B will behave just the same, carrying the full-length y of n_2, resulting in a force equal to N_2. As long as its orientation remains aligned to the principal stress directions, this setup is always at equilibrium, independently of the format (ratio of height to width) of each mesh, nor of the sign of n_1 and n_2.

[1] Our investigations suggest that we can determine a state of equilibrium for **any** arbitrary alignment of the mesh towards the PC direction. This general case will be subject of a separate publication.

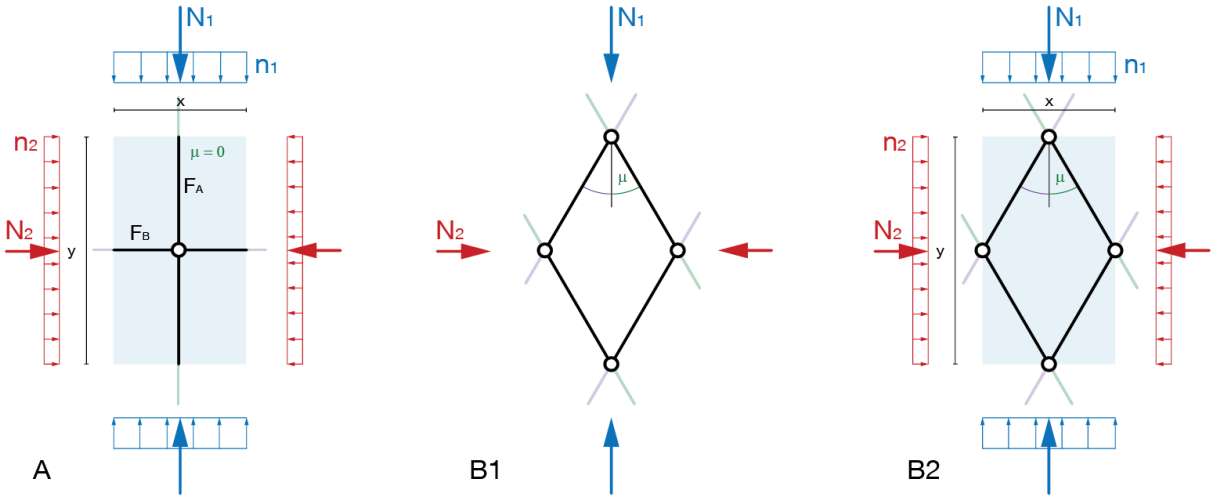

Figure 4: Orthotropic behaviour of a quadrilateral grid with point or surface loads. The grid is (A) aligned with the principal stress directions or (B) symmetric to the principal stress direction. For B an equilibrium can only be reached if N1 and N2 are of the same sign. We show the case for point loads (B1) and surface loads (B2) to illustrate the effect of surface area (x and y).

B: The edges are **symmetric to the principal stress trajectories**. In this case, there is only one angle μ that results in an equilibrium configuration. That is if the inclination of grid members corresponds to the ratio of principal stress-forces N_1 and N_2.

For a **point loads** (B1) this can simply be determined trigonometrically showing the relationship

$$F_A = \sqrt{{N_1}^2 + {N_2}^2} \tag{1}$$

$$\tan(\mu) = N_2/N_1. \tag{2}$$

Solving for μ results in:

$$\mu = \arctan(N_2/N_1) \tag{3}$$

For **surface loads** (B2), N_1 and N_2 are dependent on x and y, and are substituted:

$$N_1 = x\, n_1 \qquad \text{and} \qquad N_2 = y\, n_2 \tag{4}$$

Therefore

$$F_A = \sqrt{(xn_1)^2 + (yn_2)^2} \tag{5}$$

And

$$\tan(\mu) = \cot(\mu)(n_2/n_1) \tag{6}$$

$$\tan(\mu)^2 = (n_2/n_1) \tag{7}$$

$$\mu = \arctan\left(\sqrt{n_2/n_1}\right) \tag{8}$$

Given the principal stress values, we can deduce μ at any location and find the appropriate direction of a diagonal, principal symmetric path which will form an equilibrium layout, a D-Net. This setup is only possible for compression/tension-only shells, on which n_1 and n_2 are of the same sign, as there cannot be a negative square root in equation 8. This value for μ can be determined graphically on Mohr's circle of stress (Figure 5, B): By drawing the tangent line onto the circle from the origin, we find the ratio of equation (8). This is only possible if the circle is either left or right of the τ-axis, in other words, if n_1 and n_2 are both positive, or both negative. This correlation was found through the study of (Lisle and

Robinson 1995), who have shown a similar graphic derivation of the Gaussian curvature on a respective Mohr's circle of curvature.

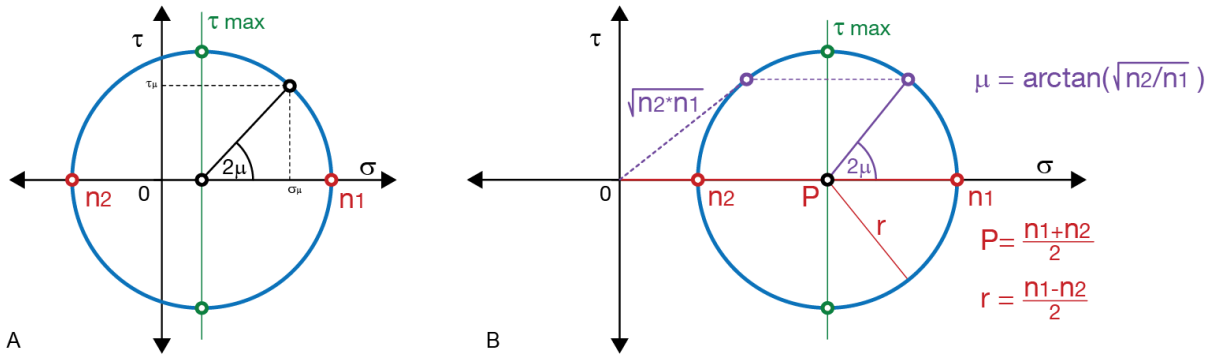

Figure 5: Mohr's circle:
A) Standard depiction displaying the relationship of stresses σ and τ in respect to the deviation μ to principal stress trajectories. The maximum shear occurs at $\mu = 45°$.
B) The D-Net directions of principal symmetric equilibrium can be determined graphically using Mohr's circle. By drawing the tangent from the origin of the system, we find 2μ on the circle.

3.2 D-Net Pathfinder using IGA

Our objective is to create an efficient digital workflow to draw the path of D-Nets on any design surface. The method is accurate enough to offer significant effects on structural performance. We use isogeometric analysis (Kiendl 2011), to allow for a continuous analysis at any point on the surface.

We use Kiwi!3D (Bauer and Längst 2019) for Rhinoceros 3D and Grasshopper, to implement the IGA on a given NURBS surface. We specify thickness, material properties and supports, and run a linear structural analysis that provides us with a displacement field. Kiwi!3D provides us with the principal stresses and directions at certain evaluation points. To trace the D-Net paths, we must be able to calculate the principal stresses at arbitrary points on the surface efficiently. Therefore we compute them directly from the deformations.

Given the undeformed and deformed shell geometry, we can calculate the stresses at any point on the surface. Therefore we compute the basis vectors A_1, A_2 in the undeformed and a_1, a_2 in the deformed configuration. The components of the stress tensor for the linear case are given by

$$\mathbf{S} = \begin{pmatrix} S_1 \\ S_2 \\ S_{12} \end{pmatrix} = \mathbf{D} \cdot \mathbf{T} \cdot \begin{bmatrix} a_1 \cdot A_1 - A_1 \cdot A_1 \\ a_2 \cdot A_2 - A_2 \cdot A_2 \\ {}^1\!/_2\,(a_1 \cdot A_2 + a_2 \cdot A_1) - A_1 \cdot A_2 \end{bmatrix}.$$

S_1 is the normal stress in the direction of the first surface parameter, S_2 the normal stress orthogonal to it and S_{12} the shear stress. $\mathbf{T}$ is the transformation matrix from the curvilinear to the Cartesian coordinate system of the surface. $\mathbf{D}$ is the stiffness of the material (Oberbichler et al. 2021). Since we are only interested in the direction and the ratio of the principal stresses, the identity matrix can be used for simplification.

The principal stresses n_1, n_2 and the corresponding directions d_1, d_2 are given by the eigenvalues and eigenvectors of the stress tensor. This way we can compute the stresses at any point on the surface and use this information to trace a specific stress path.

Pathfinder. The pathfinder is integrated with the Plugin, Bowerbird (Oberbichler 2019). It is initiated through a starting point as UV coordinate on the surface and uses formula 8 to calculate the deviation angle μ in respect to the principal stress directions. By iteratively walking along the directions and

calculating a new μ at every step, we can draw an almost smooth D-path on any shell surface. The algorithm uses the Runge-Kutta method to average out inaccuracies due to step size (Schling et al. 2017).

Negative stress ratio. If the ratio n_1/n_2 becomes negative, in other words, the two principal stresses are of opposite signs, the D-Net path naturally converges with the principal stress direction. This means, the D-path is diagonal and principal-symmetric in regions of pure compression, and parallel, principal-aligned in regions of compression and tension. In the latter, additional horizontal members have to be integrated at regular intervals to account for the horizontal stress n_2 and complete the quadrilateral network.

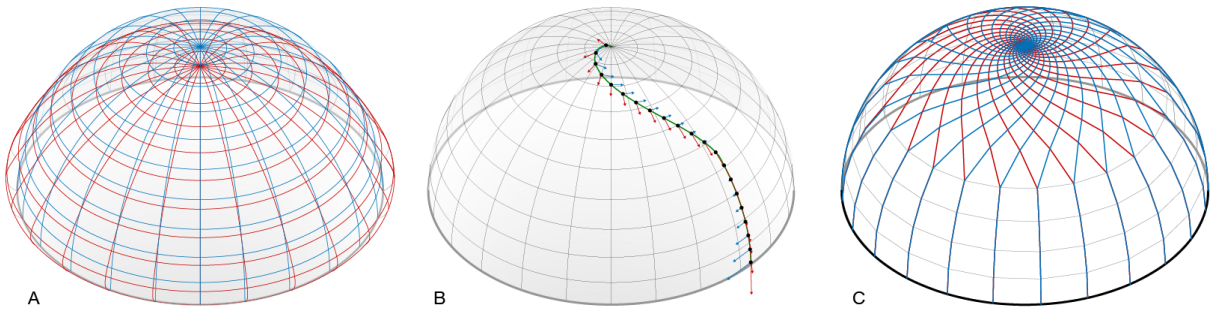

Figure 6: Computational workflow to generate D-Nets on rotational surfaces: A) We use isogeometric analysis (IGA, Kiwi3D!) to calculate the undeformed and deformed surface of the Shell and calculate the principal stress trajectories at any point. B) Our pathfinder (Bowerbird) iteratively draws a D-Curve along the surface, calculating the deviation angle at every step based on the principal stress vectors. C) We generate a discrete radial network with additional rings in areas of negative stress ratio.

Simplifications. Some practical simplifications are implemented to allow for an efficient workflow compatible with funicular form-finding and structural analysis:

- For rotational surfaces, each network is modelled with a ring at the top pole to avoid an infinitely dense layout. The loads are based on the complete self-weight of the shell and are distributed to the ring to closely resemble the load condition that originated the path.
- The IGA uses generic loads and properties, such as a poison ratio of zero, to find the accurate deformation behaviour, but not the factual numeric deflection of the shell. We are analysing the stress field of a deformed surface. Nonetheless, our pathfinder is executed on the un-deformed geometry.
- The smooth D-Net path is modelled as discrete polyline from node to node, to allow for verification of forces in our latter FE-Analysis without considering bending moments within the grid members.

4. Results and Comparison

To test the method, we first qualitatively evaluate the layout of rotational D-Nets and then compare the load-bearing behaviour of a D-Net Dome with other topologies using FE-Analysis. We conclude with an outlook on the design process.

4.1 Layout and Forces

We begin by modelling archetypical, rotational surfaces whose stress distributions are well known: a dome, a paraboloid, a cone, a cylinder and a hyperboloid (Figure 7). This allows us to assess typical effects and verify qualitatively if the layout shows the structural behaviour of meridian and ring forces.

Typically, D-Nets create a gradual shift of inclination towards the supports, where meridian compression exceeds ring compression. This effect is especially visible in the inclined cylinder (D) and at the paraboloid (B), which create low ring forces, and less pronounced at the cone (C) and hyperboloid (E), which create high compression at all heights.

Just like the analytical model of the Pantheon (Figure 2, C,D), the semi-spherical dome shows a transition from compression to tension ring at approx. 52° from the pole. Here the diagonal layout naturally transitions into the meridian direction and is replaced by a PC-layout, with additional horizontal rings. As expected, the opposite behaviour is exhibited by the hyperboloid, which displays tension on the upper three rings that are leaning outward. The typical diagonal layout appears once the ring stress becomes negative (compression).

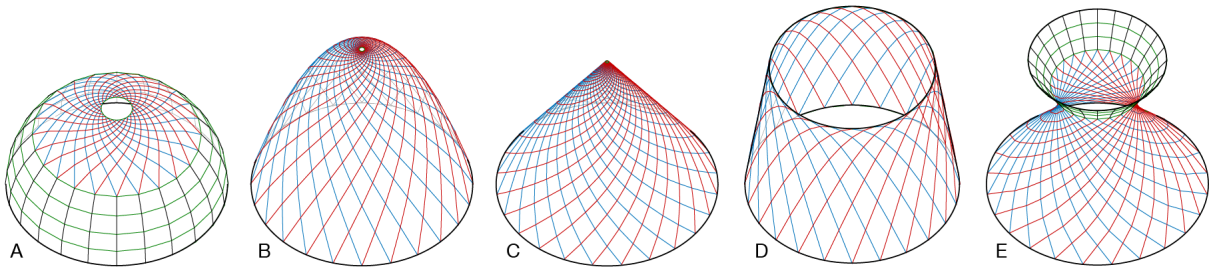

Figure 7: Examples of rotational D-Nets at equilibrium displaying the proportion of meridian and ring forces: A semi-spherical layout (A) is only possible above 52°, the paraboloid (B), cone (C) and inclined cylinder (D) offer complete D-Nets of pure compression. The Hyperboloid (E) exhibits tension rings along the top, thus pushing the D-Net to the lower half.

4.2 Structural Comparison

As a next step, we systematically compare three grid-typologies (Figure 8): A) Equilateral, B) PS-aligned and C) D-Net, to gain insight into their structural characteristics. A numerical simulation is performed to first evaluate the distribution of normal forces for four load-cases, and then conduct a modal analysis and derive tendencies of deformation.

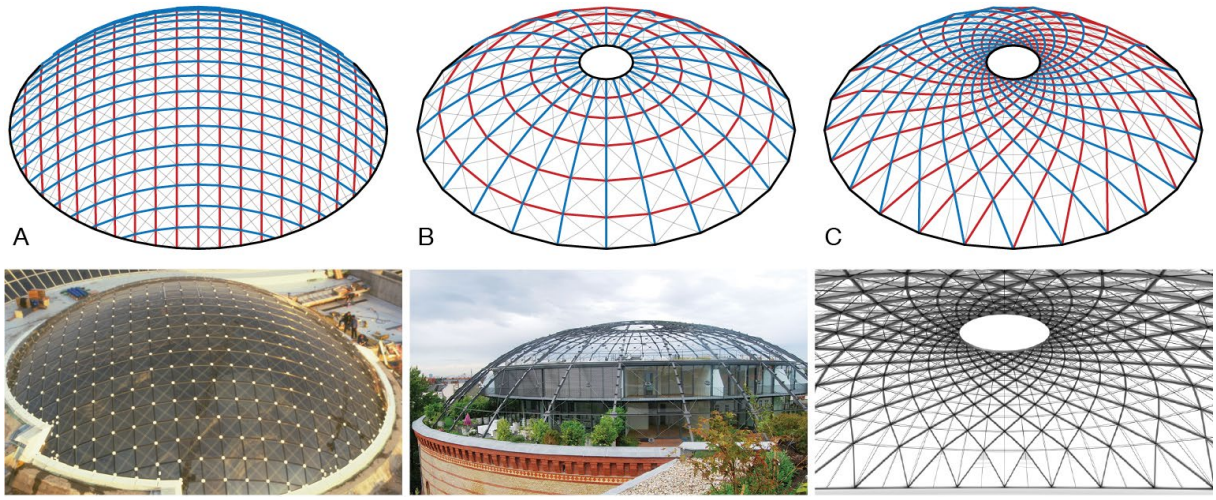

Figure 8: Spherical Gridhshells: A) Equilateral grid based on the Gridshell in Neckarsulm, B) PS- aligned network based on the Schwedler-Cupola, C) D-Net – Gridshell created for a similar spherical Surface with a uniform surface load. We show here a rendering of the possible interior.

As base surface, we choose a shallow spherical dome of radius 8 m, base diameter 12 m and height 2.9 m (within the 52° compression zone).

The **equilateral network** (A) is based on the swimming pool of Neckarsulm. The distance between the grid members is set to 0.7 m, resulting in a raster of approx. 20 x 20 meshes. The **PS-network** (B) is based on the Schwedler Cupola and divided into 24 meridian curves and 7 rings. The **D-net topology** (C) corresponds to a vertical uniform surface load and is modelled, with 24 base points resulting in 48 diagonal curves and 15 rings.

The networks are modelled discretely and each section is represented by a pin-jointed beam to exclude any bending and shear forces. We apply steel profiles, diagonal bracing, and ring supports to all networks. The section area of the profiles is constant within each grid structure but adjusted, to equalize the total mass of each gridshell ($M_{Structure} = 2300\,kg\,;\ A_{Section} = 6.0 - 8.7$ cm^2). The bracing is modelled using steel cables (tension only, Diameter = 10 mm). The Schwedler-Cupola and D-Net Structure have a bending stiff oculus of 1.75m diameter at the pole.

To simulate a realistic structural scenario, we define the following four load cases:

- G1: self-weight of the structural members (in the sum equal for all structures)
- G2: self-weight of cladding (surface load - 0.5 kN/m^2)
- W: Wind acting normal to the surface. These loads vary in each quarter from 0.4 kN/m^2 (downwind, pressure) to 0.8 kN/m^2 (transverse, suction)
- G+W: Load combination of all three scenarios (G1 + G2 + W, without safety factors)

TRA. We use the TRA*-value (inspired by the concept of force-path IL23) to quantify the load-transportation as the sum of normal forces through the structure. A low TRA*-value indicates an efficient load transfer.

$$TRA^* = \int_C N\,ds$$

The value is particularly suitable for this comparison because it is **independent of grid density** and excludes bending and shear forces, which are not relevant here. For each topology and load-case, we compute the TRA* and separate it into main structure and bracing (Figure 9, B). Together with the load-paths analysis (Figure 9 A) (showing the compressive and tensile forces in each member), we can make meaningful observations on the load-bearing behaviour:

The equilateral grid (Neckarsulm) is dependent on its bracing in any load scenario. Grid-elements that are aligned with the PS directions (meridian curves) tend to attract loads. This is especially visible in load cases G1 and G2 close to the supports. This network shows the highest TRA^* value for load-case G+W, clearly exceeding both The Schwedler-Cupola and the D-Net.

As expected, the Schwedler dome, generally shows very low TRA* values, as structural members are aligned with the principal stress directions (for G1 and G2) and efficiently transfer loads into the supports. As a result, the meridian family of beams is stressed significantly higher than the latitudinal members (ring-direction). The bracing of the Schwedler-dome is only activated when asymmetric loads are acting (W). In this case the (TRA^*) is higher than both equilateral and D-Net.

The D-net was generated for a uniform surface load. This load-case (G_2) validates our hypothesis: No bracing members are activated, allowing for a comparatively low load transportation value TRA^*. Loads are distributed symmetrically among structural members (for G1 and G2) leading to a homogeneous distribution of forces and lower local maxima when compared to the Schwedler system. For any deviation from a homogeneous surface load, the bracing is activated. This is also visible for self-weight only (G1), where the accumulation of structural members at the pole, lead to high tensile ring stress in the lower three rings. The D-Net structure performs especially well under wind load, where the diagonal layout offers efficient bracing.

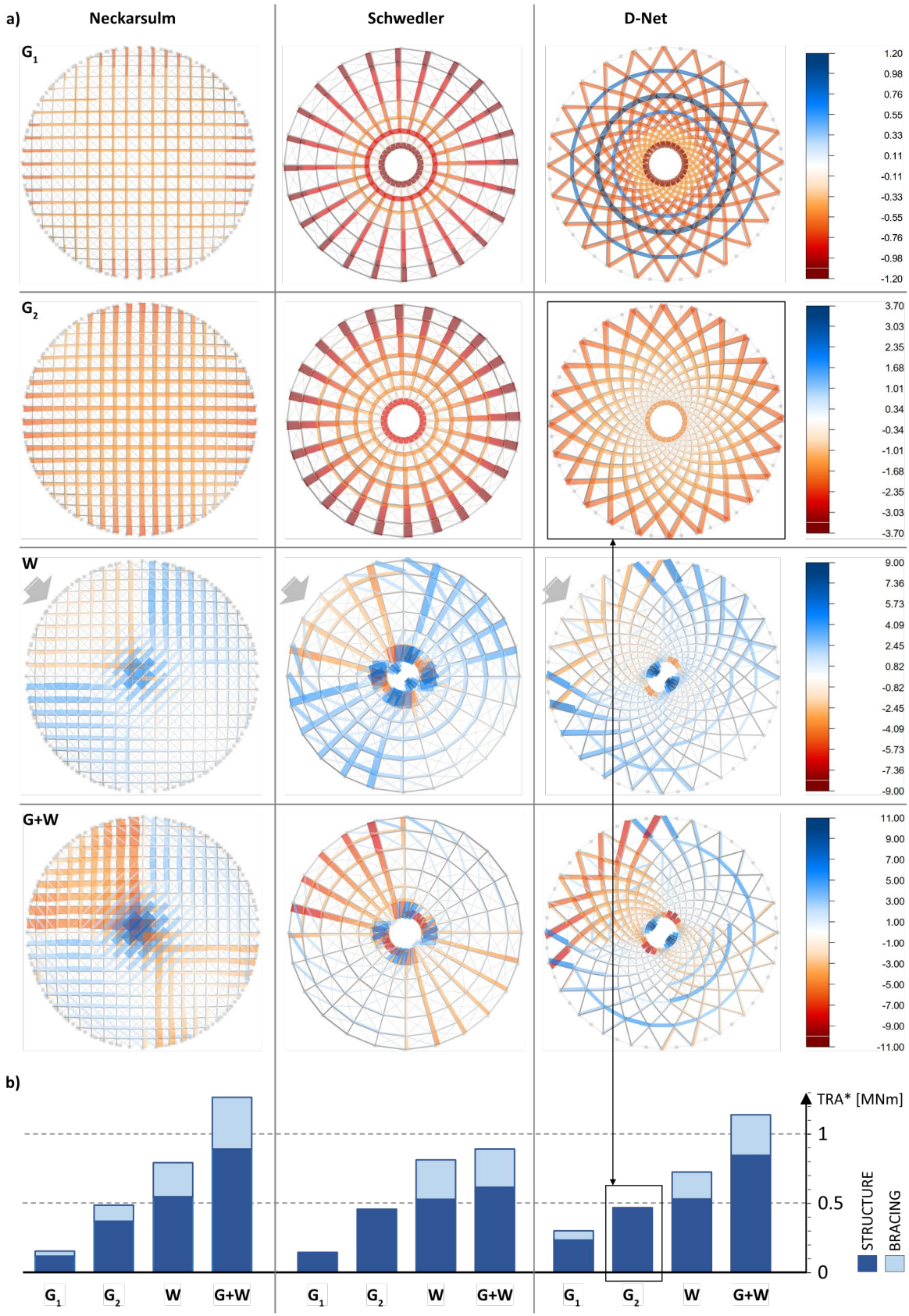

Figure 9: Results of the network-comparison: a) Normal forces, b) Load-path summation

Finally, we compute the first eigenmodes for all three structures based on self-weight and cladding (G_1 + G_2) (Figure 10). In general, all modes decisively involve a significant elongation (or fallout) of bracing, which allow a kinematic movement of the primary grid members. This mechanical behaviour is related to the ratio of stiffness (soft bracing and stiff grid) of our systems.

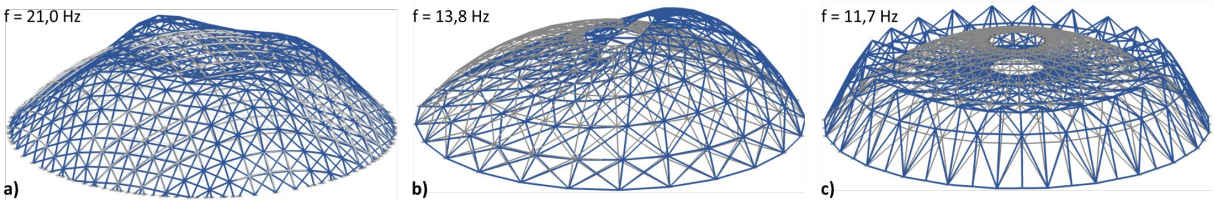

Figure 10: 1st Eigenmode and Eigenfrequencies of the equilateral network (A), the PS-aligned network (B) and the D-net (C).

The first eigenmode of the **equilateral grid** (A) creates a set of four hills and valleys aligned with the bracing direction (diagonal). This model shows the highest frequency compared to the other structures, implying a high stiffness. The **PS-aligned structure** (Schwedler dome) has an asymmetric first global eigenmode, with a distinct tilt of the upper ring. The **D-Net** deforms rotationally symmetric. The main deformation occurs in the lower area, where the rhombi show an acute angle and the bracing becomes ineffective. The D-Net how the lowest stiffness with a frequency of 11.7 Hz.

4.3 Design process

The design process, from NURBS surface to architectural grid, is not straightforward. The D-Net paths, their smoothness and regularity, are highly dependent on the load-bearing behaviour of the continuous shell. So far we have taken advantage of the rotational symmetry, as here a single D-Net path can be rotated and mirrored to generate a homogenous grid. On a freeform surface, the modelling process is more complex and must include preliminary pathfinding and post-rationalization, to include singularities and regions of positive stress ratio.

5. Conclusion

This paper presents a novel method to design equilibrium gridshells (D-Nets) symmetric to the principal stress trajectories, on any design surface. We introduce a mathematical formula for an orthotropic equilibrium of diagonal quads and implement it within a digital pathfinder on smooth NURBS surfaces using isogeometric analysis. The results are verified qualitatively along several rotational surfaces and quantitatively by comparing spherical gridshells of equilateral-, PS- and D-Net layout. The results display the potential of this novel topology, to visualize the meridian and ring forces, distribute forces equally across neighbouring members and create equilibrium states for a homogenous surface load, with minimal stress in the grid bracing.

We intend to intensify this research by implementing the digital workflow and methodology for freeform surfaces. We see great potential for the design and construction of elastic gridshells, with standardized structural elements. We further aim to develop appropriate design and construction solutions that reflect the governing load scenario. It is our goal to additionally propose D-Net solutions in regions of negative stress ratios, looking at both theoretical derivation and architectural construction.

Finally, we are also looking at discrete models in analogy to so-called S-nets (Schling et al. 2018) using the Airy stress surface to optimize quadrilateral meshes (Pellis and Pottmann 2018).

Acknowledgements

This paper is marked by a strong interdisciplinary collaboration between architects, engineers and mathematicians. We would especially like to thank Helmut Pottmann for the fruitful discussion on the correlation of mechanics and differential geometry.

Reference

Bauer, Anna M.; Längst, Philipp (2019): Kiwi3d! Meshfree, Isogeometric FE Analysis integrated in CAD. Chair of Structural Analysis, TU Munich. Available online at https://www.kiwi3d.com/, checked on 5/27/2020.

Happold, Edmund; Liddell, W. Ian (1975): Timber lattice roof for the Mannheim Bundesgartenschau. In *Structural Engineer* 1975 (53/3), pp. 99–135.

Hennicke, Jürgen (Ed.) (1974): IL10 Gitterschalen. Sonderforschungsbereich Weitgespannte Flächentragwerke. Stuttgart: Krämer (Mitteilungen des Instituts für Leichte Flächentragwerke (IL), 10).

Kiendl, Josef (2011): Isogeometric Analysis and Shape Optimal Design of Shell Structures. Dissertation. Munich.

Lisle, Richard J.; Robinson, Julian M. (1995): The Mohr circle for curvature and its application to fold description. In *Journal of Structural Geology* 17 (5), pp. 739–750.

Michalatos, Panagiotis; Kaijima, Sawako (2014): Eigenshells. Structural Patterns on modal forms. In Sigrid Adriaenssens, Philippe Block, Diederik Veenendaal, Chris J. K. Williams (Eds.): Shell structures for architecture. Form finding and optimization. London: Routledge, pp. 195–209.

Michell, A.G.M. (1904): LVIII. The limits of economy of material in frame-structures. In *The London, Edinburgh, and Dublin Philosophical Magazine and Journal of Science* 8 (47), pp. 589–597. DOI: 10.1080/14786440409463229.

Mitchell, Toby (2013): A Limit of Economy of Material in Shell Structures. Dissertation. Available online at https://escholarship.org/uc/item/0m72v2tt.

Oberbichler, Thomas (2019): Bowerbird. Blug-In for Grasshopper. Munich. Available online at https://github.com/oberbichler/Bowerbird, checked on 11/19/2020.

Oberbichler, Thomas; Wüchner, Roland; Bletzinger, K.-U. (2021): Efficient Computation of Nonlinear Isogeometric Elements using the Adjoint Method and Algorithmic Differentiation. In *Computer Methods in Applied Mechanics and Engineering*, accepted 18 March 2021.

Pellis, Davide; Pottmann, Helmut (2018): Aligning principal stress and curvature directions. In Lars Hesselgren, Karl-Gunnar Olsson, Axel Kilian, Samar Malek, Olga Sorkine-Hornung, Chris Williams (Eds.): Advances in Architectural Geometry 2018. 1. Auflage. Wien: Klein Publishing, pp. 34–53. Available online at https://www.dmg.tuwien.ac.at/geom/ig/publications/principalstress/principalstress.pdf.

Schling, Eike; Hitrec, Denis; Barthel, Rainer (2017): Designing Grid Structures using Asymptotic Curve Networks. In Klaas de Rycke, Christoph Gengnagel, Olivier Baverel, Jane Burry, Caitlin Mueller, Minh Man Nguyen et al. (Eds.): Design Modelling Symposium Paris 2017. Humanizing Digital Reality. Singapore: Springer, pp. 125–140.

Schling, Eike; Kilian, Martin; Wang, Hui; Schikore, Jonas; Pottmann, Helmut (2018): Design and Construction of Curved Support Structures with Repetitive Parameters. In Lars Hesselgren, Karl-Gunnar Olsson, Axel Kilian, Samar Malek, Olga Sorkine-Hornung, Chris Williams (Eds.): Advances in Architectural Geometry 2018. 1. Auflage. Wien: Klein Publishing, pp. 140–165.

Schling, Eike; Schikore, Jonas (2020): Asymptotic Canopy. Intergroup Hotel Ingolstadt. With assistance of Brandl Metallbau. Available online at www.eikeschling.com.

Tam, K.M.M.; Mueller, Caitlin (2015): Stress Line Generation for Structurally Performative Architectural Design. In Chris Perry, Lonn Combs (Eds.): 35th Annual Conference of the Association for Computer Aided Design in Architecture (ACADIA). Computational ecologies: Design in the Anthropocene. ACADIA. Cincinnati, pp. 94–109. Available online at http://papers.cumincad.org/data/works/att/acadia15_095.pdf.